Available online at www.sciencedirect.com
ScienceDirect
Journal of Power Sources 171 (2007) 302–309
JOURNAL OF POWER SOURCES
www.elsevier.com/locate/jpowsour

Pt/carbon nanofibers electrocatalysts for fuel cells Effect of the support oxidizing treatment

F. Zaragoza-Martín [a], D. Sopeña-Escario [b], E. Morallón [c,*], C. Salinas-Martínez de Lecea [a]

[a] *Departamento de Química Inorgánica, Universidad de Alicante, Apartado 99, E-03080 Alicante, Spain*
[b] *Fundación CIDAUT, Parque tecnológico de Boecillo, E-47151 Boecillo (Valladolid), Spain*
[c] *Departamento de Química Física e Instituto Universitario de Materiales, Universidad de Alicante, Apartado 99, E-03080 Alicante, Spain*

Received 26 February 2007; received in revised form 12 June 2007; accepted 17 June 2007
Available online 23 June 2007

Abstract

Different Pt-based electrocatalysts supported on carbon nanofibers and carbon black (Vulcan XC-72R) have been prepared using a polymer-mediated synthesis. The electrocatalysts have been characterized by transmission electron microscopy (TEM), X-ray diffraction (XRD) and cyclic voltammetry. The effect of carbon nanofibers treatment with HNO_3 solution on Pt particle size and electroactive area has been analyzed. Highly dispersed Pt with homogeneous particle size and an electroactive area around of 100 $m^2\ g^{-1}$ is obtained in raw carbon nanofibers. The oxidizing treatment of the carbon nanofibers produces agglomeration of the platinum nanoparticles and an electroactive area of 53 $m^2\ g^{-1}$. Durability studies indicate a decrease of 14% in the electroactive area after 90 h at 1.2 V in 0.5 M H_2SO_4 for platinum supported on raw carbon nanofibers and Vulcan XC-72R. The electrocatalyst supported on oxidized carbon nanofibers are stable under similar conditions.

Keywords: Pt/carbon electrocatalysts; Fuel cells; Carbon nanofibers; Characterization

1. Introduction

Low-temperature fuel cells, using either hydrogen or methanol as feed, are an efficient alternative to combustion engines in the means of transport. An important factor in the fuel cells commercialization is the catalyst cost. This cost has been reduced by using carbon-supported platinum; however, more efforts have to be done in the development of more efficient catalysts with a smaller load in precious metal. It is recognized that the form of carbon can affect the dispersion of the Pt particles [1–3]. Carbon nanofibers are such an important carbon form in the industry, and the study of the platinum dispersion on this material and its comparison with carbon black may lead to the development of improved electrocatalysts. The catalytic nanoparticles on the external walls of the carbon nanofibers (as in the case of carbon nanotubes) are easier to react with the fuel than those in the inter-particle pores of carbon black [2,4,5].

In the last decade, carbon nanotubes CNTs and nanofibers CNFs have been proposed as Pt supports for proton exchange membrane fuel cells [6–10] and direct methanol fuel cells [10–14]. Frequently, CNTs and CNFs were treated with HNO_3 acid or H_2SO_4–HNO_3 mixed acids for purification or functionalization [6,8,11]. The functionalization produces high density of oxygen-containing species on the CNT surface. The results of electrocatalytic activity in oxygen reduction reaction for Pt/CNT catalysts showed a positive effect of the fuctionalization [6]. Surface modifications of multiwalled carbon nanotubes (MWNTs) were found to be a key factor in controlling the particle size and distribution of Pt particles deposited on the MWNT support [11].

Recently, the effect of carbon supports treatment with oxidative acids in the electrocatalytic oxidation of H_2 [15] and CO [15,16] has been investigated. Treating carbon Vulcan XC-72R with HNO_3 [15], an enhancement of the amount of oxygen groups was observed. However, neither large amount of Pt, nor

* Corresponding author. Tel.: +34 965909590; fax: +34 965903537.
E-mail address: morallon@ua.es (E. Morallón).

0378-7753/$ – see front matter © 2007 Elsevier B.V. All rights reserved.
doi:10.1016/j.jpowsour.2007.06.078

better Pt dispersion was observed during the preparation of Pt/C samples. Li et al. [16] observed a wider Pt size distribution for CNTs treated with HNO_3 acid in comparison to the as received CNTs.

The objective pursued in this work was to prepare platinum-based electrocatalysts using carbon nanofibers as support. For comparative purposes electrocatalysts prepared with carbon black (Vulcan XC-72R) as support has been carried out. Furthermore, the effect of the oxidizing treatment with HNO_3 of the carbon nanofibers on the metal dispersion and catalytic activity for hydrogen oxidation has been investigated.

2. Experimental

2.1. Materials

The materials used were: hexachloroplatinic acid ($H_2PtCl_6{\cdot}H_2O$), sulfuric acid 98%, nitric acid 65%, hydrochloric acid 37%, ethylenglycol, polivinylpirrolidone (PVP) AW 40,000, Nafion solution (5%, w/w) from Aldrich, carbon black (Vulcan XC-72R) supplied by Cabot Corporation and carbon nanofibers supplied by Grupo Antolin. Water used in this work was obtained from a PureLab Elga purifier with a resistivity of 18 MΩ cm.

2.2. Carbon nanofibers treatments

Original carbon nanofibers were treated at 500 °C in N_2 flow (200 mL min^{-1} g^{-1}) during 3 h (sample denoted NF). In addition, two acid treatments were conducted on NF sample.

- Soxhlet extraction with HCl 37% during 8 h, followed by washing with water in Soxhlet for 8 h (sample denoted NF1).
- Microwave treatment with nitric acid solution. Two hundred fifty milligrams of carbon nanofibers and 10 mL HNO_3 69% were heated by MW (570 W) for 35 min. The sample was washed after treatment with water in Soxhlet for 8 h (sample denoted NF2).

Both treated materials were dried after treatment in a conventional oven at 120 °C overnight.

2.3. Electrocatalysts preparation

The experimental procedure for the electrocatalysts preparation is based on the method described by Chen and Xing [17]. This method is a reduction-by-solvent type, which involves using PVP to achieve small and uniform platinum particles. The solvent used was an ethylene glycol–water mixture in a volume ratio 3:1. Theoretical platinum content in the catalysts was fixed in 20%. Some modifications were introduced in order to make this method suitable for carbon nanofiber supports. The support was previously dispersed in ethylene glycol, with the aim to improve the fiber–solvent contact. The Pt precursor (hexachloroplatinic acid) was added as a solution (1 wt% Pt). The prepared catalyst was washed with acetone and ultra pure water instead of ethanol, since the latter may contaminate the platinum surface.

The catalysts notation is Pt/support name.

2.4. Characterization

Ash content in carbon supports was determined by thermogravimetry (TG) in air (80 mL min^{-1}) flow, heating the sample from 25 to 920 °C (heating rate: 10 °C min^{-1}) using a thermobalance Stanton Redcroft STA-780. TEM images were obtained using a JEOL microscope (model JEM-2010). The X-ray diffraction (XRD) equipment used was a Seifer JSO-Debyeflex 2002. Temperature programmed desorption (TPD) of carbon supports were carried out using a thermobalance SDT TA Instruments 2960, coupled to a mass spectrometer Balzers MSC 200 Thermostar (heating rate: 20 °C min^{-1}; gas flow: He, 100 mL min^{-1}).

To determine the metal content, 0.1 g of the catalyst were digested with 20 mL H_2SO_4 (98%) and 10 mL HNO_3 (65%). The suspension was heated at 573 K (under reflux) until a clear solution was obtained (after about 24 h). After solvent evaporation, 1 mL HNO_3 (65%) and 3 mL HCl (37%) were added. The obtained solution was transferred into a 100 mL calibrated flask and the volume completed with deionized water. The solutions were then analyzed using inductively coupled plasma atomic emission spectroscopy (ICP-AES), Perkin-Elmer Optima 3000 and 4300.

X-ray photoelectron spectroscopy (XPS) of the catalysts was carried out by means of a spectrometer VG-Microtech Multilab, using Mg Kα (1253.6 eV) radiation from a double anode with an energy flow of 50 eV.

For the cyclic voltammetry (CV) measurements a three-electrode electrochemical cell was used. The reference electrode was a reversible hydrogen electrode (RHE), whereas a spiral-rolled platinum wire was used as the counter electrode. The equipment used for the voltammetric measurements was an EG&G potentiostat (model 263A). For the voltammetric characterization, 5 μL of dispersion of the powder samples were deposited on a glassy carbon surface of a 3 mm of diameter previously sanded and cleaned with water. The support dispersions were made using 8 mg of the carbon nanofibers and 1 mL of acetone, whereas for the catalysts dispersions in acetone and Nafion (5%, w/w) solution were used. The concentration of the catalysts dispersions was 10 mg mL^{-1}, and Nafion content (as solid) was 33% of the total solid content (catalyst + Nafion). All dispersions were homogenized in an ultrasonic bath for at least 40 min.

3. Results and discussion

3.1. Characterization of the carbon nanofibers

Table 1 shows the ash content (in weight percentage) of the carbon supports. As already known, Vulcan XC-72R has very low ash content. In carbon nanofibers, the ash content is mainly constituted of the metal compounds used in their synthesis. It can be observed that treatment with HNO_3 completely removes these

Table 1
Ash content, quantification of oxygen surface groups by TPD and XPS analysis for all carbon supports

Carbon support	Ash (wt%)	TPD			XPS		
		CO (μmol g^{-1})	CO_2 (μmol g^{-1})	%O	%C	%O	O/C
NF	7.9	166	2603	8.6	95.6	3.8	0.04
NF1	2.6	0	1042	3.3	95.1	3.8	0.04
NF2	0	331	4512	15.0	90.8	9.2	0.10
Vulcan XC-72R	0	0	677	2.2	91.7	8.0	0.08

compounds, whereas the treatment with HCl is not so effective in metal removal. Table 1 also shows the quantification of the TPD experiments and the XPS analysis of the samples. These carbon materials contain mainly groups desorbing as CO_2. According to literature [18] they correspond to carboxylics, lactones and anhydrides. Acid treatments modify the amount of these groups in the carbon nanofibers. The oxygen content estimated from the amount of $CO + 2CO_2$ (μmol g^{-1}) is included in Table 1. HCl reduces the oxygen content while HNO_3 considerably increases the oxygen surface groups. The oxygen content results from XPS again show that sample NF2 has the higher value. However, for the other samples some differences are observed in comparison to TPD results. The values for NF and NF1 are similar while sample Vulcan XC-72R having the lower value from TPD presents much higher oxygen content. The apparent discrepancy among TPD and XPS results must be a consequence of the depth limitation of XPS analysis while oxygen from TPD corresponds to the sample bulk. The differences observed from both techniques are a consequence of the different distribution of oxygen groups in the carbon materials.

The NF materials are highly graphitic, stacked-cup-type carbon nanofibers having a wide hollow core, without amorphous carbon coatings [19]. The oxidizing treatment produces oxygen groups at the edges of graphitic planes, increasing the number of defects at the surface.

Fig. 1 shows the steady voltammograms obtained for the carbon supports in 0.5 M H_2SO_4 solutions. As it can be seen, samples NF, NF1 and Vulcan XC-72R mainly show capacitative behaviour when cycling between −0.3 and 1.2 V (dotted lines in Fig. 1a, b and d). In the case of sample NF2, in the same potential range, shows a clear reversible peak around 0.65 V related to the existence of oxygen surface groups as consequence of the HNO_3 treatment. When cycling up to 1.6 V, the steady voltammograms of samples NF and NF1 change becoming similar to that of NF2, since surface oxygen groups are being created due to electrochemical oxidation. The voltammogram for Vulcan XC-72R support also shows an increase in the current after oxidation up to 1.6 V, but this increase is lower than for the NF and NF1 samples. Contrarily, when the potential increases to 1.6 V, the voltammogram shape of sample NF2 does not change signif-

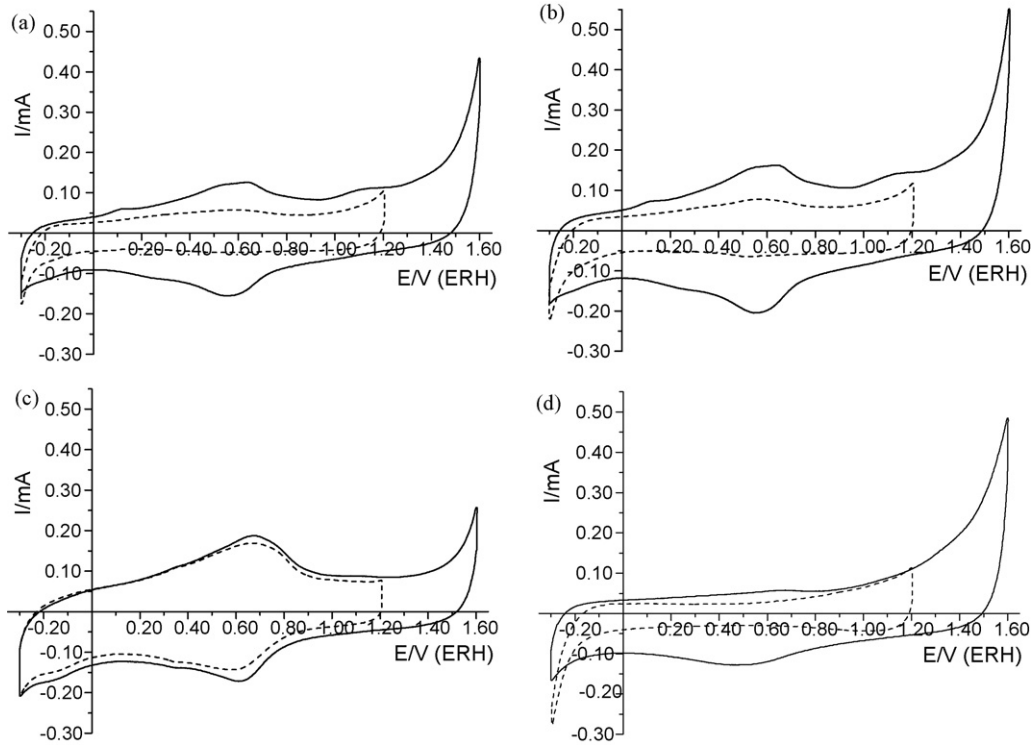

Fig. 1. Cyclic voltammogram for the different carbon supports at (- -) 1.2 V and (–) 1.6 V. (a) NF, (b) NF1, (c) NF2 and (d) Vulcan XC-72R. 0.5 M H_2SO_4 solution; 50 mV s^{-1}.

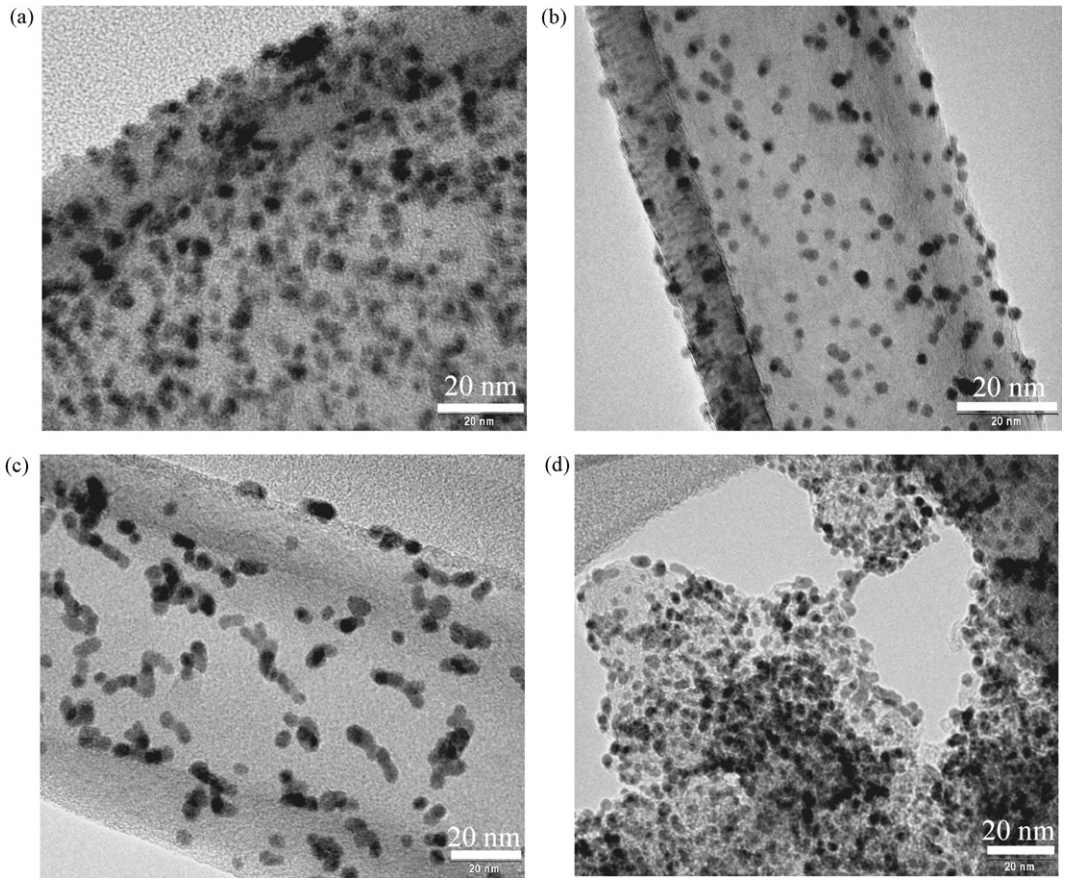

Fig. 2. TEM images of platinum nanoparticles on: (a) Pt/NF, (b) Pt/NF1, (c) Pt/NF2 and (d) Pt/Vulcan XC-72R.

icantly showing the redox couple in the same potential range. Then, the electrochemical treatment in NF2 sample does not produce additional surface oxygen groups at these conditions.

Then, the characterization of the carbon nanofibers indicates that HCl acid removes most metal content without creating surface groups. HNO_3 acid treatment provides the formation of oxygen surface groups as well as removal of the initial metal content, the important amount of surface oxygen groups producing the redox processes in the voltammogram. NF1 and NF samples show a very similar electrochemical behaviour.

3.2. Characterization of the Pt electrocatalysts

3.2.1. Physicochemical characterization

Fig. 2 shows the TEM images of the different Pt electrocatalyts showing a uniform distribution of the platinum particles on the carbon surface. Pt particles are also very uniform in size. However, as observed in Fig. 2c the metal particles in sample Pt/NF2, although not very different in diameter compared to other samples, are agglomerated forming long clusters. The metal particle size distribution in the supported catalysts was obtained by measuring the size of ~1000 randomly chosen particles in the magnified TEM images. For sample Pt/NF2, considering the particular shape of the clusters, the criterion used for particle sizing was the average of diameter and length. Fig. 3 shows the histograms obtained for the four platinum supported catalysts. The average diameters obtained (included in Table 2) are 3.4, 2.7 and 2.6 nm for Pt/NF, Pt/NF1 and Pt/Vulcan XC-72R respectively, which are accompanied by a relatively narrow particle size distribution (1–5 nm). The polymer-mediated synthesis [17] facilitates the formation of small and uniform Pt particles on the different carbon nanofibers supports. However, for the Pt/NF2 catalyst the average size is larger and also the particle size distribution is wider than for the other supports. Fig. 4 shows the powder XRD patterns for the different platinum supported electrocatalysts. The clear diffraction peak at 26.3° in carbon nanofibers is associated with the (0 0 2) graphitic planes. The graphitic structure of the carbon nanofibers wall is also observed in the micrograph of Fig. 2b. Contrarily, the crystallinity of sample Vulcan XC-72R is very poor. All the electrocatalysts display the characteristic patterns of Pt fcc diffraction. The 2θ values of the (1 1 1), (1 0 0) and (1 1 0) peaks appear at around 39.6°, 46.0° and 67.7°, respectively, for all the catalysts. The broader

Table 2
Platinum nanoparticle sizes measured by different techniques

Catalyst	TEM (nm)	DRX (nm)	Cyclic voltammetry (nm)
Pt/NF	3.4	2.4	3.3
Pt/NF1	2.7	2.2	2.9
Pt/NF2	5.2	3.5	5.4
Pt/Vulcan XC-72R	2.6	2.0	3.1

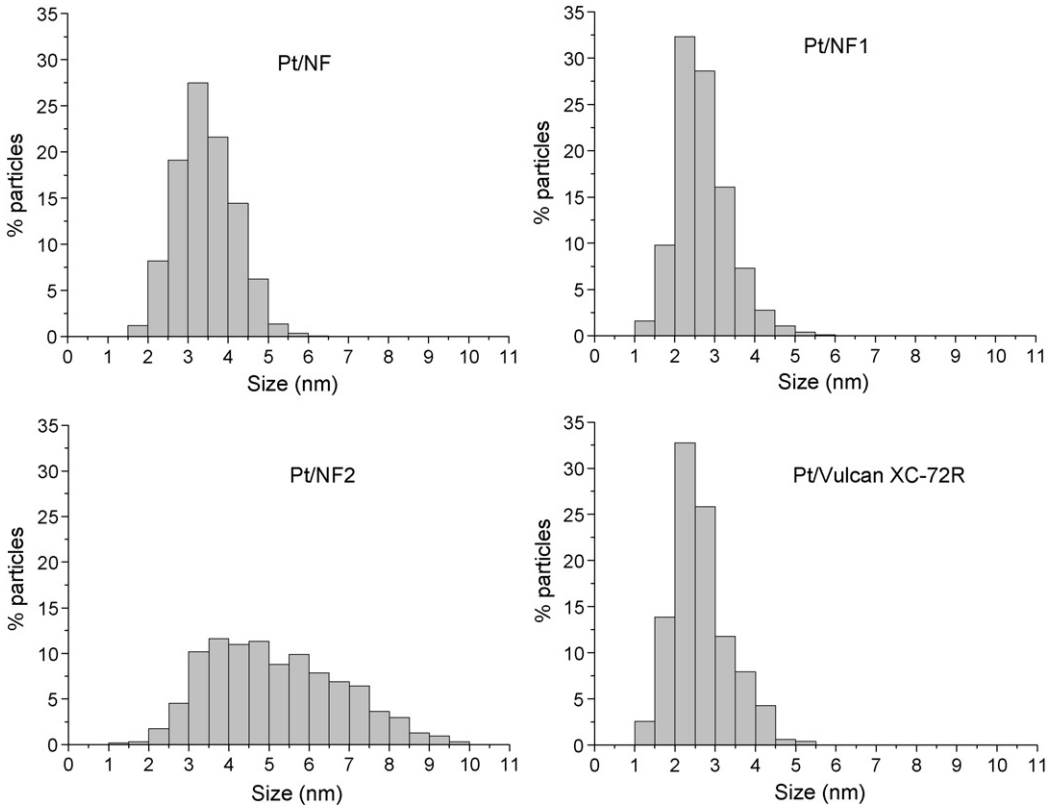

Fig. 3. Histograms of Pt particle size distribution on Pt/NF, Pt/NF1, Pt/NF2 and Pt/Vulcan XC-72R catalysts.

diffraction peaks for the Pt/NF, Pt/NF1 and Pt/Vulcan XC-72R led to smaller average particle size as calculated by the Scherrer equation [20]. Table 2 compares the estimated average size of the platinum particles for the different electrocatalysts obtained by TEM and DRX. The values obtained with both techniques are in good agreement with the exception of sample Pt/NF2. As stated previously, the method used for TEM particle sizing in this sample introduces some arbitrary decisions resulting in the impossible comparison with average crystal size from XRD. In any case, XRD confirms that the platinum particle size is higher for the Pt/NF2 catalyst. Thus, the oxidizing treatment with HNO_3 facilitates the platinum nanoparticles agglomeration. As already mentioned the oxidizing treatment produces oxygen groups and creates defects at the surface of the carbon nanofibers. The surface oxygen groups or defects on the carbon nanofibers surface probably act as anchorage sites for Pt particles. The long clusters observed in catalyst Pt/NF2 must be a consequence of the surface oxygen groups or defects distribution at the nanofibers surface. A similar effect can be found in the literature, although this fact is not mentioned by the authors [16]. Pt supported in multiwall carbon nanotubes treated in HNO_3 and $H_2SO_4 + HNO_3$ solutions exhibit agglomeration of Pt particles not present in the as received CNTs.

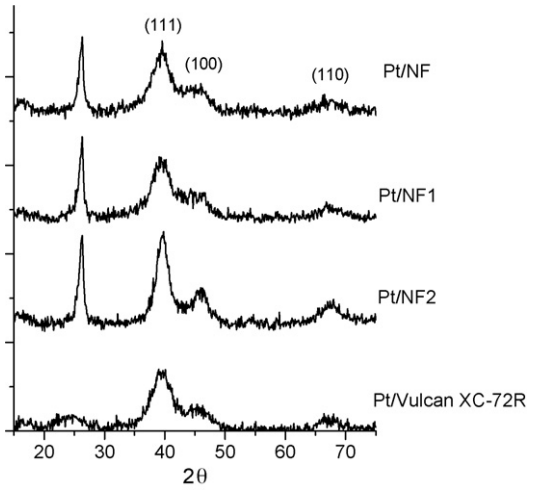

Fig. 4. X-ray diffraction patterns of Pt/carbon-supported catalysts.

XPS has been used to determine the surface oxidation states of the platinum. Table 3 shows the percentage of Pt and Pt(II) detected in the metal surface. As it can be seen, some amount of oxidized platinum was found in all samples. This fact is not unusual as the samples were prepared and dried in air. When comparing these values with those for the particle size, it can be seen that the percentage of Pt(II) increases when the particle size decreases. Table 3 also shows the amount of platinum measured by ICP showing that the amount of platinum in all the samples is around 20-wt% in agreement with the theoretical amount in the sample preparation.

3.2.2. Electrochemical characterization

Fig. 5 shows the steady voltammograms for the different electrocatalysts in 0.5 M H_2SO_4 solutions. It can be clearly observed the characteristic profile for a platinum electrode

Table 3
Characterization of the different prepared Pt/carbon catalyts: Pt content by XPS and ICP and electroactive surface areas

Catalyst	% Pt(0)	% Pt(II)	Pt (wt%) (ICP)	Electroactive surface area ($m^2\ g^{-1}$ Pt)
Pt/NF	79.6	20.4	20.6	86
Pt/NF1	72.9	27.1	20.2	96
Pt/NF2	81.5	18.5	22.1	53
Pt/Vulcan XC-72R	70.4	29.6	21.8	90

in the potential range between 0.05 and 0.4 V, corresponding to the adsorption–desorption processes (hydrogen and anion adsorption–desorption) on the platinum surface, and in the potential range between 0.75 and 1.2 V corresponding to the formation of surface platinum oxide. The electrical charge measured between 0.05 and 0.4 V can be used (after doing the double layer correction) for the determination of the surface active area of platinum considering that the value of 210 $\mu C\ cm^{-2}$ corresponds to the adsorption of one electron per surface platinum atom. Table 3 shows the platinum electroactive surface area (S_{Pt}) of the catalysts referred to the grams of platinum. The results are very similar for samples Pt/NF, Pt/NF1 and Pt/Vulcan XC-72R which have an electroactive area of $91 \pm 5\ m^2\ g^{-1}$ Pt. This value is among the higher found in literature [10,16,17]. However, sample Pt/NF2 shows much lower electroactive area (nearly half of that for sample Pt/NF1).

The platinum particle size in nanometres (diameter, nm) can be calculated from the electroactive surface area (S_{Pt}) assuming that this value is the ratio between the area and the weight of one Pt particle of spherical shape (Eq. (1)):

$$d = \frac{6000}{\rho_{Pt} \times S_{Pt}} \quad (1)$$

where ρ_{Pt} is the platinum density ($21.4\ g\ cm^{-3}$).

The values obtained from the voltammetric results are presented in Table 2. A very good agreement exits between the particle size obtained from cyclic voltammetry the other two techniques (TEM and DRX), showing that the electroactive surface area has been properly measured and no contamination of the platinum surface exists.

3.2.3. Stability test

The electrocatalysts have been tested at 1.2 V during long period time in 0.5 M H_2SO_4 solution. Fig. 6 shows the electroactive surface area determined by cyclic voltammetry plotted against the time at 1.2 V. It can be observed that the Pt/Vulcan XC-72R and Pt/NF catalysts show a very similar behaviour with a decrease of 14% after 90 h. The electroactive surface area of

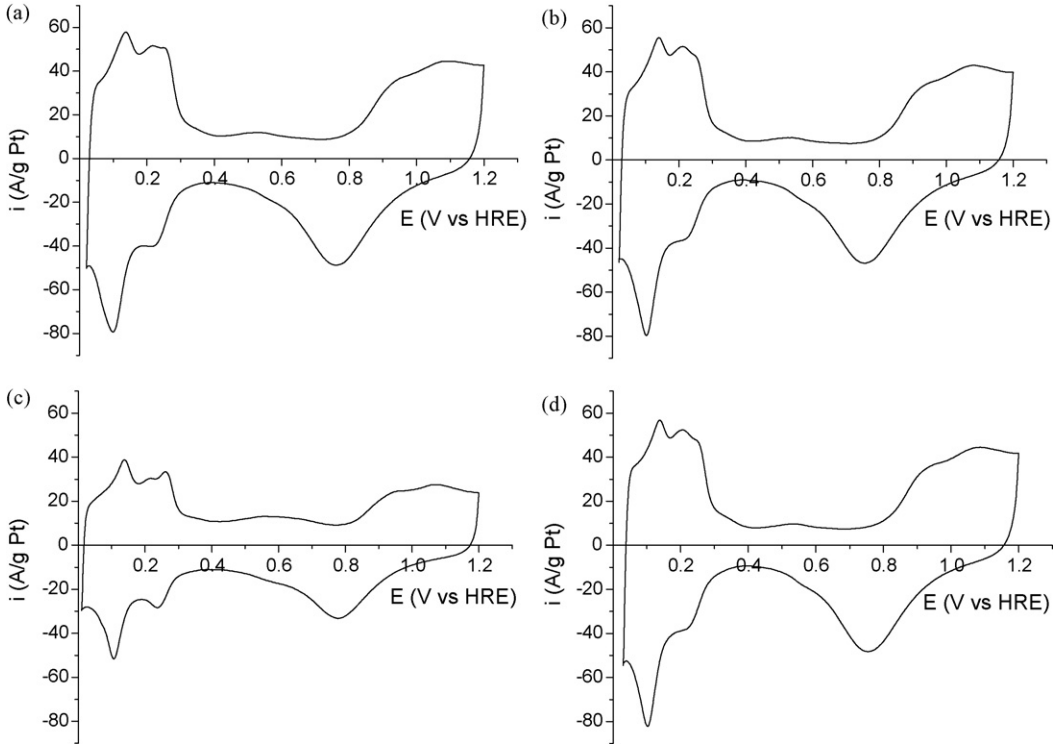

Fig. 5. Steady cyclic voltammograms of the different Pt/carbon catalysts at 1.2 V. (a) Pt/NF, (b) Pt/NF1, (c) Pt/NF2 and (d) Pt/Vulcan XC-72R. 0.5 M H_2SO_4 solution; 50 mV s^{-1}.

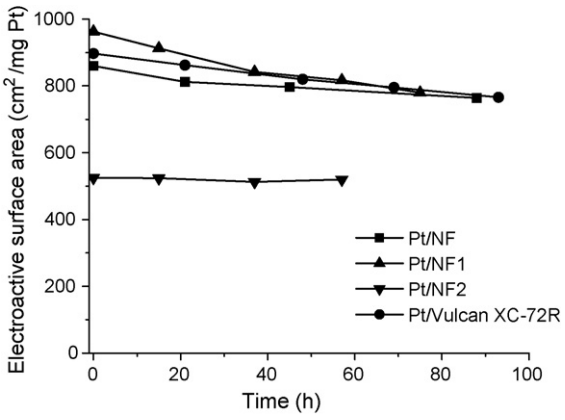

Fig. 6. Plots of electroactive surface areas versus test time at 1.2 V in 0.5 M H_2SO_5 solution for the different Pt/carbon catalysts.

Pt/NF1 decreases a 19% after 75 h. The Pt/NF2 catalyst shows a better stability than the others catalysts however its electroactive surface area is considerably lower. The results obtained for us are better than those obtained for other authors in the same conditions using carbon black and carbon nanotubes as catalysts supports [21]. These authors show a decrease of 35.2 and 20.2% for the Pt/Vulcan XC-72 and Pt/CNTs, respectively, after 95 h in the same experimental conditions. The decrease in the electroactive area can be ascribed to several factors like Pt particle size growth, the oxidation of the carbon support, and Pt dissolving into the solution. The TEM images (Fig. 7) show a sintering of the platinum particles as the main reason of the decrease in the electroactive surface area. Then, the oxidation of the carbon support by electrochemical treatment favours the platinum nanoparticles aggregation. Then, for electrocatalysts supported on carbon nanofibers a direct relation is found between stability and oxygen content of the support (see Table 1). The lower stability is for sample Pt/NF1 while the highest is for Pt/NF2.

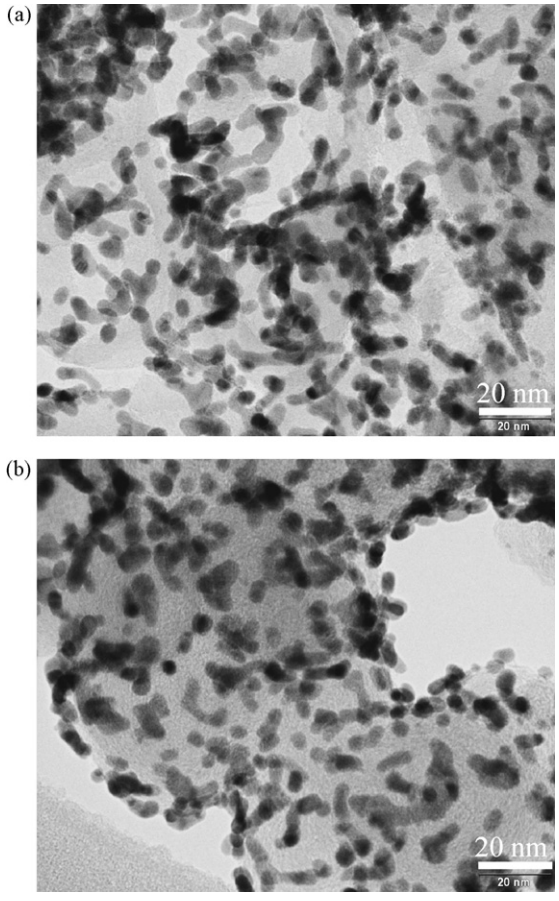

Fig. 7. TEM images after 165 h at 1.2 V in 0.5 M H_2SO_5 solution for: (a) Pt/NF and (b) Pt/Vulcan XC-72R catalysts.

4. Conclusions

A polymer-mediated synthesis of platinum nanoparticles supported on carbon nanofibers have been used for the electrocatalysts preparation. Several techniques have been used for the characterization of the support and the electrocatalysts. This synthesis method produces highly dispersed Pt nanoparticles on the carbon nanofibers with an average diameter around 2.5 nm. The electroactive surface areas obtained with the nanofiber supports (NF and NF1) are similar to that obtained with carbon black (Vulcan XC-72R) and near to 100 $m^2\ g^{-1}$ Pt. However, the oxidizing treatment of the nanofibers produces oxygen groups and creates defects on the carbon nanofibers acting as anchorage sites for Pt particles. Thus, the oxidizing treatment favours the aggregation of the platinum nanoparticles considerably reducing the electroactive surface area. Electrocatalysts supported on carbon nanofibers exhibits a stability at 1.2 V in sulfuric acid solution similar to Pt/Vulcan XC-72R. The slight decrease in the electroactive surface area results from Pt particle aggregation that can be produced by the effect of the applied potential and the electrochemical oxidation of the carbon support.

Acknowledgement

The authors would like to thank Grupo Antolín Ingeniería S.A. for providing sample GANF.

References

[1] A.L. Dicks, J. Power Sources 156 (2006) 128–141.
[2] T.R. Ralph, M.P. Hogarth, Platinum Met. Rev. 46 (3) (2002) 117–135.
[3] E. Antolini, L. Giorgi, F. Cardellini, E. Passalcqua, J. Solid State Electrochem. 5 (2001) 131–140.
[4] J. Xu, K. Hua, G. Sun, C. Wang, X. Lv, Y. Wang, Electrochem. Commun. 8 (2006) 982–986.
[5] D. Villers, S.H. Sun, A.M. Serventi, J.P. Dodelet, S. Désilets, J. Phys. Chem. 110 (2006) 25916–25925.
[6] Z. Liu, X. Lin, J.Y. Lee, W. Zhang, M. Han, L.M. Gan, Langmuir 18 (2002) 4054–4060.
[7] C. Wang, M. Waje, X. Wang, J.M. Tang, R.C. Haddon, Y. Yan, Nanoletters 4 (2004) 345–348.
[8] F. Yuan, H.K. Yu, H. Ryu, Electrochim. Acta 50 (2004) 685–691.
[9] M. Gangeri, G. Centi, A. La Malfa, S. Perathoner, R. Vieira, C. Pham-Huu, M.J. Ledoux, Catal. Today 102-102 (2005) 50–57.
[10] M. Carmo, V.A. Paganin, J.M. Rosolen, E.R. Gonzalez, J. Power Sources 142 (2005) 169–176.
[11] W. Li, C. Liang, W. Zhou, J. Qiu, Z. Zhou, G. Sun, Q. Xin, J. Phys. Chem. B 107 (2003) 6292–6299.
[12] G. Che, B.B. Lakshmi, Ch.R. Martin, R. Ellen, Langmuir 15 (3) (1999) 750–758.

[13] Z. He, J. Chen, D. Liu, H. Zhou, Y. Kuang, Diam. Relat. Mater. 13 (2004) 1764–1770.
[14] H. Tang, J. Chen, L. Nie, D. Liu, W. Deng, Y. Kuang, S. Yao, J. Colloid Interface Sci. 269 (2004) 26–31.
[15] J.L. Gomez de la Fuente, S. Rojas, M.V. Martinez-Huertas, P. Terreros, M.A. Peña, J.L.G. Fierro, Carbon 44 (2006) 1919–1929.
[16] L. Li, G. Wu, B.-Q. Xu, Carbon 44 (2006) 2973–2983.
[17] M. Chen, Y. Xing, Langmuir 21 (2005) 9334–9338.
[18] Y. Otake, R.G. Jenkins, Carbon 31 (1993) 109.
[19] I. Martin-Gullon, J. Vera, J.A. Conesa, J.L. González, C. Merino, Carbon 44 (2006) 1572–1580.
[20] B.E. Warren, X-ray Diffraction, Addison-Wesley, Reading, MA, 1996.
[21] Y. Shao, G. Yin, Y. Gao, P. Shi, J. Electrochem. Soc. 153 (6) (2006) A1093–A1097.